Causal strategy for set-membership fault diagnosis

Stéphane Ploix, Sylviane Gentil

Laboratoire d'Automatique de Grenoble, INPG, UJF, UMR 5528,
BP 46, F-38402 Saint Martin d'Hères Cedex, France
Phone: 33 4 76 82 62 28, Fax: 33 4 76 82 63 88
e-mail : Stephane.Ploix@inpg.fr, Sylviane.Gentil@inpg.fr

Abstract. Set-membership fault detection seems to be a promising approach because it takes into account a priori knowledge on modelling uncertainties and measurement errors. It consists in coherency tests with measurements and models. Nevertheless, a careful diagnostic strategy has to be designed in order to achieve fault diagnosis of complex processes. To achieve the diagnostic procedure, a causal analysis allows focusing the coherency tests on simple models, resulting in a decrease of the amount of computations. This paper will present an application to a nuclear waste treatment plant. The proposed causal strategy for diagnosis will be explained first. The set-membership coherency tests will be justified. Finally, a fault scenario will be presented in order to enlighten the method.

Keywords. Causal reasoning, fault detection and isolation, model-based diagnosis, set membership test.

I. Introduction

Fault diagnosis is a very active research area and a lot of different methods have been suggested to tackle this problem. Artificial Intelligence proposes a logical framework for diagnosis and Poole (1989) distinguishes two kinds of reasoning to solve diagnostic tasks: *normal-operation-oriented reasoning* and *abnormal-operation-oriented or abductive reasoning*. Nevertheless, whatever the reasoning is, any diagnostic procedure is always based on coherency tests between observations and a behavioural model. Diagnostic procedures differ in the type and the nature of models and in the way the coherency tests are performed. Models may represent a normal pattern of behaviour or an abnormal one, when dedicated to a specific fault (Travé-Massuyès et al, 1997). They may be qualitative or quantitative, composed by a set of signatures or by relations between physical variables.

Independently of the type of procedures involved, diagnosis resides in the conclusions drawn from coherency tests: the behaviour in question is akin to the reference behaviour or not.

In theory, an incoherence between observed and reference behaviour induces that the actual behaviour does not match the reference behaviour and consequently that the process state does not match the reference state. Conversely, in the event of coherency, the only possible conclusion is that the process state may be similar to the reference state because faults may exist without persistently affecting behaviour at all operating modes. It is nevertheless clear that a coherency maintained during different operating modes reinforces the hypothesis of identity between reference and actual process state.

Numerical model based diagnosis leads to particular ways of testing coherency among data. Nevertheless, a difficult issue when using precise numerical models is to make the difference between data incoherence due to a real fault in the system or due to noise disturbing measurements and to model imprecision. Several tools are used to solve this problem, such as testing hypothesis in a probabilistic framework, fuzzy modelling of errors (Evsukoff et al, 2000), etc. More recently, set membership calculus has been used and seems to be a promising approach because it takes into account a priori knowledge on modelling uncertainties and measurement errors (Ploix, 1998).

In any case, model-based diagnosis raises problems in practice if the system to diagnose is very complicated, because methods that work fine for a model with two or three variables may well be completely useless in this case. Causal reasoning is another useful tool issued from artificial intelligence approaches to process analysis. It appears to be a suitable solution to avoid the numerical model based diagnostic complexity because it allows focusing the coherency tests on simple sub-models and thus it results in the decrease of the amount of computations. Furthermore this reasoning mechanism has implicit explanatory properties that are essential when diagnosis is envisaged as a human operator support system.

This paper shows the possibility of a causal strategy for set-membership fault diagnosis. The first section presents the process under study: a nuclear waste treatment plant. The second section explains the proposed causal strategy for diagnosis. The set-membership coherency tests will be justified in section three. At last, a fault scenario will be presented in section four in order to enlighten the method and finally a conclusion will be given.

II. The process

An application of the method was carried out at a nuclear fuel reprocessing plant (figure 1) designed to separate

uranium and plutonium from fission products (FP) by selective extraction. The plant is composed of two pulsed columns coupled head to tail. In the following, a single column is presented to simplify the explanation. A pulsed column is a liquid-liquid extraction device. The spent fuel (comprising uranium, plutonium and FP) is dissolved in nitric acid (CQ0500), and the extraction column selectively transfers uranium and plutonium to an organic phase (inlet CQ1010 and outlet QG600). Most of the fission products remain in the aqueous phase (QE120).

The extraction step requires that the aqueous and organic phases be thoroughly mixed to maximise the contact surface area between the two solvents and thereby optimise the chemical exchange phenomena. The column is thus subjected to periodic pressure pulses (CPRE801) to form an emulsion in order to delay the descent of the heavy phase and to mix it with the light phase. The interface – the surface physically separating the two phases – is located in the settler at the bottom of the column (NIRE), and is regulated by drawing off the aqueous phase (QE120) at a suitable rate.

A simulator of the process is available and consists in a set of non-linear differential equations. It is based on a deep mathematical model of the plant, written by nuclear physicists. It can provide reference behaviour and can simulate faulty behaviour too (sensor, actuator and process faults). It has been designed to train operators to control and supervise the plant in various situations. In the following, and for evident safety reasons, the experiments which are presented are obtained with this simulator and not with a real faulty process.

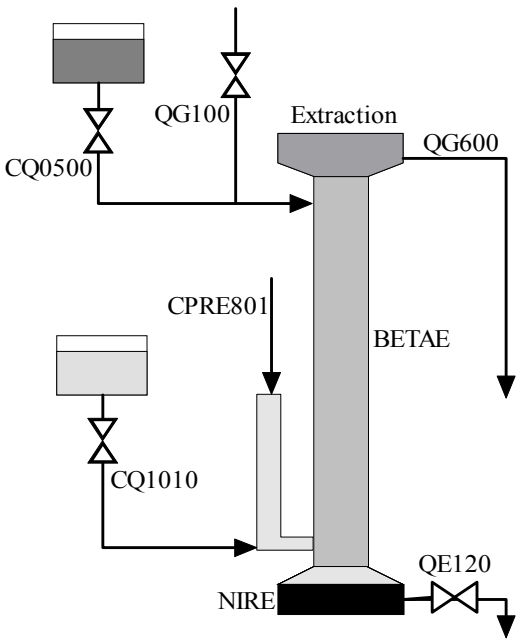

Figure 1. The pulsed column

III. Causal strategy for diagnosis

In Artificial Intelligence, Causal Reasoning is relative to the analysis of system behaviour in terms of cause-and-effect relationships between entities characteristic of its state, e.g. variables or alarms. A causal structure is an abstract description of the influences some variables have on other ones (Davis, 1983).

The behaviour of any device may be partially described by a causal graph, composed of unidirectional relationships between variables. Arcs that symbolise functional relationships link them. $x \rightarrow y$ means that the state of y at time t depends on the state of x at time $t'<t$; x is the cause, y the effect. As a consequence, transcribing normal behaviour models in terms of directed causal graphs provides a graphical tool to reason about the physical laws governing the device. The nodes are the variables relevant to the required abstraction level and the arcs represent the directed causal relationships between them. The implicit principle is that this structure then provides a conceptual tool for reasoning about the way in which normal but also abnormal changes propagate within a plant or how they may be explained; this principle yields as long as the causal relationships are not modified by given failures.

An important point is that a causal model is qualitative, thus adapted to various modelling possibilities. An arc can represent the simple knowledge that a relation between two variables exists. Signs can label the directed arcs if the input and output signal trend relations are known. The arcs can also be parameterised using basic concepts of control engineering theory and thus they are related to classical transfer functions. The causal graph of the system is thus a special representation of block-diagrams, where all variables are measured and the block transfer functions are as simple as possible.

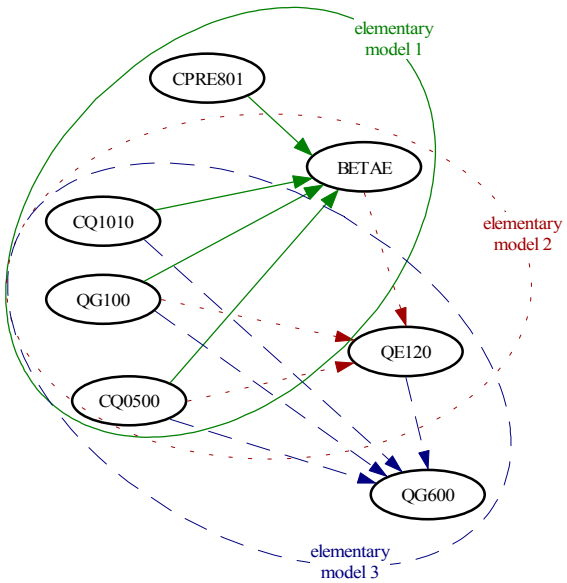

Figure 2. A simplified causal graph

A causal model is declarative; thus it is completely independent of the algorithms using it, such as simulation,

explanation, diagnosis or action advice. For diagnostic purposes, forward and backward chaining in the graph allows analysis from a fault to its consequences and from symptoms to their possible causes.

In practical cases the causal graph is not necessarily easy to develop, and requires a detailed physical analysis but this, in turn, is the source of its explanatory capability. A careful physical analysis of the process under study has resulted in a causal graph linking input and output flows, levels and column weights (Leyval et al. 1994).

A simplified graph is proposed in figure 2. It corresponds to the highest abstraction graph of the nuclear fuel reprocessing application. The causal graph of the complete process includes 45 variables with 9 setpoints and 5 control-loops.

IV. Set-membership coherency test.

Many works in the literature have dealt with coherency principle for the past 15 years or so. De Kleer and Williams (1987) proposed a particularly interesting methodology. Their work only applies to deterministic static systems, but its interest resides in the fact that they formulate the diagnostic problem by introducing the principle of coherency and exoneration. Chow and Willsky (1984), followed by Massoumnia and Van der Velde (1988) introduced parity space techniques. These techniques, which are especially well suited to sensor fault detection, usually rely on the hypothesis that the system model is certain. When the model is uncertain, these techniques attempt to reject model uncertainties. In an other way, Patton et al (1989) developed approaches based on state observers, but just like the previous ones, these approaches reject uncertainties as unknown inputs instead of taking them into consideration: it results that the ensuing coherency tests mainly concern the certain parts of the process. The Kalman filter is an exception here, because it includes vectors of stochastic variables and helps to determine, automatically, the thresholds depending on noise standard deviation. The uncertainties appearing in the models used by Kalman filters have an additive structure, which can only lead to invariant thresholds on residuals in the stationary case. Only few researchers have shown an interest on techniques taking uncertainties into consideration (Horak and Allison, 1990; Adrot et al, 1999; Armengol et al, 2000).

About ten years ago, lots of works formulating identification problems in a membership context appeared (Walter and Piet-Lahanier, 1987; Norton, 1987; Clément and Gentil, 1988; Schweppe, 1973). Instead of representing the uncertainties by Gaussian stochastic variables, these approaches--also known as bounding approaches--represent the uncertainties by a set of possible values, where only the bounds are known. Theses works have been collected in a collective volume that presents the main results (Milanese et al, 1996). But these works have barely got beyond the parameter estimation theory context.

In this article, we describe a technique using the bounding approach for the diagnosis of uncertain systems. In order to perform the ineluctable coherency tests, it now remains for us to take a look at what they become when behavioural models involve uncertainties. The basic principle of this approach has been described in (Ploix et al, 2000) and it will not be developed in this paper which is dedicated to an application of bounding approach to a class of complex dynamical systems.

The model of the pulsed column, whose structure is given by the causal graph in figure 2, is composed of 3 elementary models MISO. Each model can be decomposed into several arcs; each one corresponds to a transfer function of one of the following type: gain with time delay, 1st order transfer function with time delay, derivative with gain and 1st order transfer function with derivative and time delay…. Each parameter of the transfer functions is supposed to belong to a bounded set represented by an interval, except for the uncertainties on time delay which are supposed to be smaller than the sample time and, consequently, negligible.

Noting $\mathcal{A}(\upsilon)$, the bounded set of all the possible values of υ, a first order transfer function with parameter uncertainties may be written as follows:

$$\frac{dy}{dt} = -\frac{1}{(1+\rho_\tau \upsilon_\tau)\tau} y + \frac{(1+\rho_k \upsilon_k)k}{(1+\rho_\tau \upsilon_\tau)\tau} u \qquad (2a)$$

where $\rho_\tau \geq 0$, $\rho_k \geq 0$ and $\mathcal{A}(\upsilon_\tau) = \mathcal{A}(\upsilon_k) = [-1\ 1]$.

It means that there is respectively ρ_τ% and ρ_k% of uncertainty on τ and k. Moreover, measurement white noises have to be modelled. Noting $\tilde{y}$, the measurement of the physical variable y, the equation (2a) must be completed by:

$$\tilde{u} = u + \rho_u \upsilon_u \text{ and } \tilde{y} = y + \rho_y \upsilon_y \qquad (2b)$$

where $\rho_u \geq 0$, $\rho_y \geq 0$ and $\mathcal{A}(\upsilon_u) = \mathcal{A}(\upsilon_y) = [-1\ 1]$.

Model (2) takes into account 4 different uncertainties; nevertheless, it cannot be directly used: only discrete-time models can be utilised. Assuming that uncertain variables do not vary during a sample time, a discrete time model can be evaluated. If u comes from a zero order hold, model (2) yields

$$\begin{cases} y_{k+1} = e^{-\frac{T_e}{(1+\rho_\tau \upsilon_\tau)\tau}} y_k + k(1+\rho_k \upsilon_k)\left(1 - e^{-\frac{T_e}{(1+\rho_\tau \upsilon_\tau)\tau}}\right)\tilde{u}_k \cdots \\ \qquad \cdots - k(1+\rho_k \upsilon_k)\left(1 - e^{-\frac{T_e}{(1+\rho_\tau \upsilon_\tau)\tau}}\right)\rho_u \upsilon_u \\ \tilde{y}_k = y_k + \rho_y \upsilon_y \end{cases} \qquad (3)$$

To calculate $\mathcal{A}(y_k)$ $\forall k$, the expression (3) will be simplified by assuming that uncertainties are small enough to be represented by a first order Taylor expansion around $\upsilon_i = 0$ $\forall i$. The result appear in table 1. Whatever the transfer function type without derivative is, the discrete-time model may be written in the form:

continuous-time transfer function	discrete-time model whose structure is given by (7a) (line 1 and 2) or by (7b) (line 3 and 4)					
	a	a_τ	b	b_τ	b_k	e_u
$\frac{(1+\rho_k \upsilon_k)k}{1+(1+\rho_\tau \upsilon_\tau)\tau p}$	$e^{-\frac{T_e}{\tau}}$	$\frac{T_e e^{-\frac{T_e}{\tau}}}{\tau}\rho_\tau$	$k\left(1-e^{-\frac{T_e}{\tau}}\right)$	$-\frac{kT_e e^{-\frac{T_e}{\tau}}}{\tau}\rho_\tau$	$k\left(1-e^{-\frac{T_e}{\tau}}\right)\rho_k$	$k\left(1-e^{-\frac{T_e}{\tau}}\right)\rho_u$
$(1+\rho_k \upsilon_k)k$	0	0	k	0	$k\rho_k$	$k\rho_u$
$\frac{(1+\rho_k \upsilon_k)kp}{1+(1+\rho_\tau \upsilon_\tau)\tau p}$	$e^{-\frac{T_e}{\tau}}$	$\frac{T_e e^{-\frac{T_e}{\tau}}}{\tau}\rho_\tau$	$\frac{k}{\tau}$	$-\frac{kT_e e^{-\frac{T_e}{\tau}}}{\tau}\rho_\tau$	$\frac{k}{\tau}\rho_k$	$\frac{k}{\tau}\rho_u$
$(1+\rho_k \upsilon_k)kp$	0	0	k	0	$k\rho_k$	$k\rho_u$

Table 1. Relation between continuous-time uncertain models and discrete-time models

$$\begin{cases} y_{k+1} = (a + a_\tau \upsilon_\tau) y_k + (b + b_\tau \upsilon_\tau + b_k \upsilon_k)\tilde{u}_k + e_u \upsilon_u \\ \tilde{y}_k = y_k + \rho_y \upsilon_y \end{cases} \quad (4a)$$

If there is a derivative, the discrete-time model structure is:

$$\begin{cases} y_{k+1} = (a + a_\tau \upsilon_\tau) y_k + (b + b_\tau \upsilon_\tau + b_k \upsilon_k)(\tilde{u}_{k+1} - \tilde{u}_k)\cdots \\ \qquad \cdots + e_u(\upsilon_{k+1} - \upsilon_k) \\ \tilde{y}_k = y_k + \rho_y \upsilon_y \end{cases} \quad (4b)$$

Table 1 collects the resulting model for each arc type (Fagarasan, 2000).

To compute the set of all possible values of the measurement $\tilde{y}_k$, the following interval calculation laws (Moore, 1979) have to be used. Let υ_1, υ_2 and θ be three independent uncertain variables satisfying $\mathcal{A}(\upsilon_1)=\mathcal{A}(\upsilon_2)=[-1,1]$, $\mathcal{A}(\theta)=\left[\breve{\theta},\hat{\theta}\right]$ and λ_1, λ_2 be two deterministic variables belonging to 0, the following properties may be easily proven:

- if $\forall\theta\in\left[\breve{\theta},\hat{\theta}\right]$, $\forall\upsilon_1\in[-1,1]$, $\frac{\partial f(\theta,\upsilon_1)}{\partial\theta}\geq 0$ then

$$\mathcal{A}\left(f(\theta,\upsilon_1)\right)=\left[\inf_{\upsilon_1\in A(\upsilon_1)}\left(f\left(\breve{\theta},\upsilon_1\right)\right),\ \sup_{\upsilon_1\in A(\upsilon_1)}\left(f\left(\hat{\theta},\upsilon_1\right)\right)\right] \quad (5a)$$

$$-\ \mathcal{A}(\lambda_1+\lambda_2\upsilon_2)=\left[\lambda_1-|\lambda_2|,\lambda_1+|\lambda_2|\right] \quad (5b)$$

$$-\ \mathcal{A}(\lambda_1\upsilon_1+\lambda_2\upsilon_2)=\left[-|\lambda_1|-|\lambda_2|,|\lambda_1|+|\lambda_2|\right] \quad (5c)$$

Thanks to these three properties, it is easy to compute the set of all possible values of $\tilde{y}_k$: $\mathcal{A}(\tilde{y}_k)$. Property (5a) is satisfied because the function giving y_{k+1} is strictly rising $\forall$ $y_k\in\mathcal{A}(y_k)$:

$$\frac{\partial y_{k+1}}{\partial y_k} = a + a_\tau \upsilon_\tau \approx a > 0$$

The abstract space $\mathcal{A}(\tilde{y}_k)$ is obtained by solving one of the two following systems depending of the presence of derivative. From (4a):

$$\begin{cases} \mathcal{A}(y_0)=[\breve{y}_0,\hat{y}_0] \\ [\breve{y}_{k+1},\hat{y}_{k+1}]=\begin{bmatrix} a\breve{y}_k + b\tilde{u}_k - |a_\tau\breve{y}_k + b_\tau\tilde{u}_k| - |b_k\tilde{u}_k| - |e_u|, \\ a\hat{y}_k + b\tilde{u}_k + |a_\tau\hat{y}_k + b_\tau\tilde{u}_k| + |b_k\tilde{u}_k| + |e_u| \end{bmatrix} \\ \mathcal{A}(\tilde{y}_k)=\left[\breve{y}_k-\rho_y,\hat{y}_k+\rho_y\right] \end{cases} \quad (6a)$$

and from (4b):

$$\begin{cases} \mathcal{A}(y_0)=[\breve{y}_0,\hat{y}_0] \\ [\breve{y}_{k+1},\hat{y}_{k+1}]=\begin{bmatrix} a\breve{y}_k + b(\tilde{u}_{k+1}-\tilde{u}_k) - |a_\tau\breve{y}_k + b_\tau(\tilde{u}_{k+1}-\tilde{u}_k)|\cdots \\ \quad \cdots - |b_k(\tilde{u}_{k+1}-\tilde{u}_k)| - |e_u|, \\ a\hat{y}_k + b(\tilde{u}_{k+1}-\tilde{u}_k) + |a_\tau\hat{y}_k + b_\tau(\tilde{u}_{k+1}-\tilde{u}_k)|\cdots \\ \quad \cdots + |b_k(\tilde{u}_{k+1}-\tilde{u}_k)| + |e_u| \end{bmatrix} \\ \mathcal{A}(\tilde{y}_k)=\left[\breve{y}_k-\rho_y,\hat{y}_k+\rho_y\right] \end{cases} \quad (6b)$$

Now, the coherency test can be performed by verifying that

$$\tilde{y}_k \in \mathcal{A}(\tilde{y}_k) \quad (7)$$

If (7) is satisfied, the observations are coherent with the model.

The causal graph of figure 2 reveals that the global model of the nuclear fuel reprocessing plant is composed of 3 interconnected elementary models. Diagnostic procedures may be based on two or three of these models connected with each other. It is thus important to be able to connect uncertain models. Thanks to the calculation laws (5), it is possible by substituting the set of all possible outputs $[\breve{y}_k,\hat{y}_k]$ of the upstream model to the known input $\tilde{u}_k$ of the downstream model.

From a practical view, the uncertainty characteristics have to be determined. There are two main approaches: an empirical one and a numerical one. The first one consists in utilising physical knowledge on uncertainties and then in adjusting the additive uncertainties (e_u in table 1) in order for the normal behaviour remains coherent with models used. The second one that has been used for this work consists in using algorithms given in (Ploix et al, 1999).

Models used for coherency test	Sensors checked							Equivalent behaviour checked		
	CPRE801	CQ1010	QG100	CQ0500	BETAE	QE120	QG600	EM1	EM2	EM3
EM1	Yes	Yes	Yes	Yes	Yes	No	No	Yes	No	No
EM2	No	Yes	Yes	Yes	Yes	Yes	No	No	Yes	No
EM3	No	Yes	Yes	Yes	No	Yes	Yes	No	No	Yes
EM1+EM2	Yes	Yes	Yes	Yes	No	Yes	No	Yes	Yes	No
EM2+EM3	No	Yes	Yes	Yes	Yes	No	Yes	No	Yes	Yes
EM1+EM2 +EM3	Yes	Yes	Yes	Yes	No	No	Yes	Yes	Yes	Yes

Table 2. All possible coherency tests and corresponding sensors and sub-processes checked

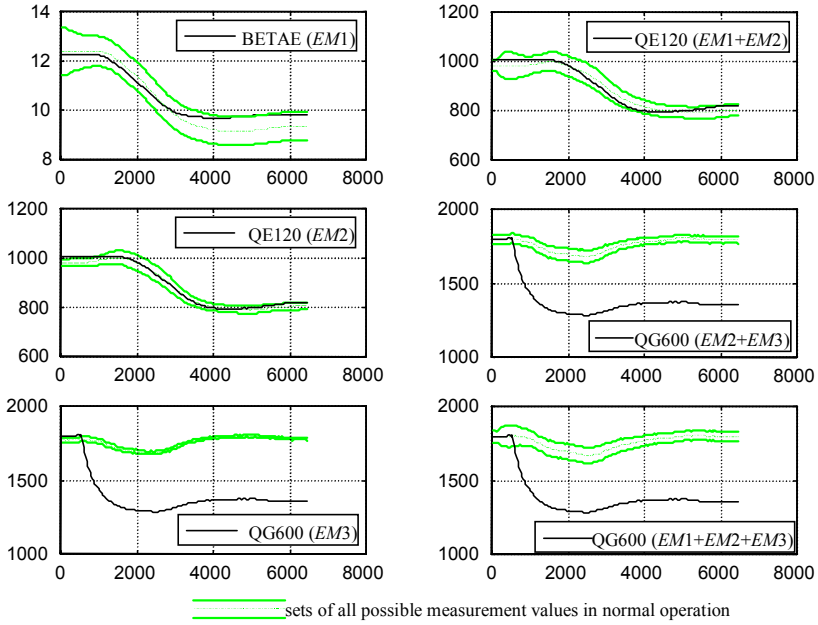

Figure 3. Coherency tests in case of sensor fault on QG600 at 500 s.

V. Diagnostic strategy and fault scenario

A new normal-operation-oriented strategy has been settled. Its main principle relies on the fact that any coherency test covers both process and sensor behaviour. The coherency tests based on the elementary models *EM*1, *EM*2, *EM*3 (figure 2) check the process behaviour in the deepest way, but they are not sufficient to distinguish faults on the process from sensor faults. Thus, complementary tests based on models combining two or three elementary models have to be proceeded. These models are supposed to have a single measured output, the one of the downstream model. Table 2 is deduced from the causal graph in figure 2; it sums up the sensors and sub-process behaviour checked by coherency tests based on the different possible models.

Figure 3 represents the results obtained when a fault occurs on QG600 sensor. The obtained intervals are time varying i.e. it amounts to adaptive thresholds a priori determined by the uncertainty characteristics. When looking at estimated QG600 envelopes given by models *EM*3, *EM*2+*EM*3 and *EM*1+*EM*2+*EM*3, it can be observed that chaining up models does not lead to important increases of uncertainties on model outputs.

Coherency tests are not satisfied for models *EM*3, *EM*2+*EM*3 and *EM*1+*EM*2+*EM*3, and satisfied for the others. The sensors and behaviours covered by models leading to incoherence have to be suspected. Table 2 reveals that all the sensors and all the states of sub-processes have to be suspected. Now, the satisfied coherency tests have to be considered: for all sensors and models covered by these tests have to be exonerated. As tests based on models *EM*1, *EM*2 and *EM*1+*EM*2 are coherent, all sub-processes and all sensors are exonerated excet QG600 sensor.

Note that the first step of the strategy is sure whereas the second one has to be confirmed during different operating modes. The final diagnostic is thus that there is one or more faults among sensors and sub-processes, and that a fault on QG600 sensor seems to be the origin of the incoherences.

VI. Conclusion

Causal analysis seems to be a relevant tool to achieve set-membership diagnostic strategies. The abstraction of causal graph points out the process structure that induces the nature of coherency tests and then the diagnostic

strategy presented in this paper. The proposed diagnostic approach provides a new tool for fault diagnosis of a class of complex dynamical uncertain systems. The approach can be easily extended to abnormal-operation reasoning (only the reference model is changed) and thus, it gathers fault detection and fault isolation tasks in a same framework.

The strategy can be improved by taking into account time propagation, transient nature of incoherences. Coherency tests can also be improved to provide more precise diagnosis. It is indeed easy to calculate the distance between the measurement $\tilde{y}_k$ and the closest bound of the domain $\mathcal{A}(y_k)$ to appreciate the level of coherency.

Acknowledgements.

We thank J. Montmain, engineer at the French Nuclear Central Agency (Commissariat à l'Énergie Atomique, Unité de recherche sur la complexité EMA-CEA, site EERIE, Nîmes) for providing data and models of the process and for fruitful discussions about operation support and causal reasoning.

We thank I. Fagarasan, PhD student in Facultatea de Automatica si Calculatoare at Universitatea Politehnica Bucuresti, Romania, for her help in implementing the application to the process and for providing results appearing on figure 3.

VII. References

Adrot 0., D. Maquin, J. Ragot., 1999, Fault detection with model parameter structured uncertainties, European Control Conference ECC'99, Karlsruhe.

Armengol J., J. Vehi, L. Travé-Massuyès, M.A. Sainz, 2000, Interval Model-based fault detection using multiple sliding time windows, 4th symposium on Fault Detection Supervision and Safety for Technical Processes, Budapest.

Chow E.Y., A.S. Willsky, 1984, Analytical redundancy and the design of robust failure detection systems, IEEE trans. Autom. Contr., AC-29, pp. 603-614.

Davis R., 1983, Diagnosis via causal reasoning : paths of interaction and the locality principle, Amer Ass Artif Int, pp. 88-94.

De Kleer J., 1987, Diagnosing multiple faults, Artificial Intelligence, 32, pp. 97-130.

A. Evsukoff, S. Gentil, J. Montmain, 2000, Fuzzy Reasoning In Co-operative Supervision Systems, Control Engineering Practice, 8, pp. 389-407.

Clément Th., S. Gentil, 1988, Reformulation of parameter Identification with unknown but bounded errors, Mathematics and computers in simulation, 30, pp. 257-270.

Fagarasan I., 2000, Diagnostic des défaillances avec une approche ensembliste et un raisonnement causal, Rapport interne du Laboratoire d'Automatique de Grenoble, France.

Horak D.T., B.H. Allison, 1990, Failure detection and isolation methodology, Proc. of the American Control Conference, pp. 2955-2958.

Leyval L., S. Gentil and S. Feray-Beaumont, 1994, "Model based causal reasoning for process supervision", Automatica, 30 (8), pp. 1295-1306.

Massoumnia M.M., W.E. Van der Velde, 1988, Generating parity relations for detecting and identifying control system component failures, Journal of guidance, control and dynamics, 11(1), pp. 60-65.

Milanese M., J. Norton, H. Piet-Lahanier, E. Walter (ed.), 1996, Bounding approaches to system identification, Plenum Press, New-York and London.

Moore R.E., 1979, Methods and applications of interval analysis, SIAM, Philadelphia, Pennsylvania.

Norton J.P., 1987, Identification and application of bounded-parameter models, Automatica, 4, pp. 497-508.

Patton R.J., P. Frank, R. Clark (Ed.), 1989, Fault diagnosis in dynamic systems, Prentice Hall, International series in systems and control engineering.

Ploix S., 1998, Diagnostic des systèmes incertains : l'approche bornante, Phd of the National Polytechnic Institute of Lorraine (INPL).

Ploix S., O. Adrot, J. Ragot, 2000, Bounding approach to the diagnosis of a class of uncertain static systems, SAFEPROCESS 2000, Budapest, Hungary.

Ploix S., O. Adrot, J. Ragot, 1999, Parameter Uncertainty Computation in Static Linear Models, Conference on Decision and Control, Phoenix, U.S.A., pp. 1916-1921.

Poole D., 1988, Normality and faults in logic-based Diagnosis, International Joint Conference on Artificial Intelligence, Detroit, Michigan USA, 1304-1310, 20-25.

Schweppe F.C., 1973, Uncertain dynamic systems, Prentice Hall, Englewood Cliffs, N.J, U.S.A.

Travé-Massuyès L., P. Dague P., F. Guerrin, 1997, Le raisonnement qualitatif, Hermès, Paris.

Walter E., H. Piet-Lahanier, 1987, Exact and recursive description of feasible parameter set for bounded error models, 26th IEEE Conf. on Decision and Control, Los Angeles, pp. 1921-1922.